

Unveiling the photostability of the molecule of colour shikonin: From solution to the solid state

C.M. Pinto^a, C. Clementi^{b,*}, F. Sabatini^{c,1}, I. Degano^d, A. Romani^b, J.S. Seixas de Melo^{a,*}

^a University of Coimbra, CQC-IMS, Department of Chemistry 3004-535 Coimbra, Portugal

^b University of Perugia, Department of Chemistry, Biology and Biotechnology, Perugia, Italy

^c Institute of Chemical Science and Technologies "G. Natta" (CNR - SCITEC), Perugia, Italy

^d University of Pisa, Department of Chemistry and Industrial Chemistry, Pisa, Italy

ARTICLE INFO

Keywords:

Photochemistry
Photodegradation
Shikonin
Natural dyes
Naphthoquinones
Molecules of colour

ABSTRACT

Shikonin, **Shk**, is a molecule of colour characterized by its natural phenolic-based compound composition, belonging to the naphthoquinone family. It is known for its low solubility in water and limited resistance to lightfastness. **Shk** is present in variable amount in the dried roots of *Lithospermum erythrorhizon*, *Lithospermum officinale*, and *Alkanna tinctoria*. The dyestuff extracted from these plants has historically been employed in Asia and Europe for textile dyeing, producing various shades of purple. Despite the historical significance of this dye, it has received limited attention in the context of cultural heritage studies. In the present work, **Shk** and model hydroxynaphthoquinone dyes were irradiated with polychromatic and monochromatic light in solution and in the solid state, mimicking paint mock-ups, to evaluate their photochemical stability. Low photoreaction quantum yield values ($\phi_R < 10^{-5}$) were observed in solution, providing quantitative evidence for the high stability of this molecule to light exposure. Chromatographic-mass spectrometric analyses carried out on the irradiated solutions and extracts from artificially aged **Shk** paint mock-ups, detected 5,8-dihydroxy-2-(1-hydroxy-3-oxo-4-methyl-4-pentenyl)-1,4-naphthoquinone as degradation product, together with newly identified intermediate species involved in the complex photodegradation process. These indicate that, both in solution and in the solid state, the photoreaction of **Shk** proceeds with a similar mechanism. In the context of heritage science, this work contributes to highlight the potentialities of the adopted noninvasive approach, corroborated by results collected by chromatographic-mass spectrometric techniques, in identifying **Shk** in historical and archaeological specimens through its absorption and emission features and/or by detecting its degradation products which are, for the first time, characterized in terms of their UV-Vis absorption and emission spectral properties.

1. Introduction

Shikonin is a purple dye present as a primary colored component in the extracts from the dried roots of *Lithospermum erythrorhizon*, also known as gromwell [1-4]. The habitat of this plant is situated in China, Korea, Russia, and Japan. Shikonin is also found in another plant, *Alkanna tinctoria*, which is native to Central Europe and Mediterranean region [5]. However, *Alkanna tinctoria* contains a smaller amount of dyeing material and, in addition to shikonin, also includes the R-enantiomer of **Shk**, known as alkannin [6,7].

The extract from gromwell roots produces a deep purple dyestuff that has been extensively used from ancient times in many Asian regions, for

dyeing silk with beautiful colors ranging from lilac to violet [6]. Known as *zi cao* dye, it was popular in China as far back as the Warring States era (circa 475–221 BCE) [8-10]. In Japan, in the Nara period (710 – CE 794), only the royal family and the highest ranking officials were allowed to use the extract of the gromwell roots, known as *murasaki* dye, as a source of violet for dyeing silk [10]. Analytical studies based on chromatographic techniques have identified the presence of this dye in historical textiles, and in particular in a Japanese *manchira* [11], in a Chinese purple stripe from the Tang Dynasty (618 – CE 907) [12] and in various samples dated back to the 19th century collected in Western countries, where it was known as “Tokyo violet” [6,12]. Despite there is no experimental evidence on the exploitation of **Shk** as a pigment, its use in

* Corresponding authors.

E-mail addresses: catia.clementi@unipg.it (C. Clementi), sseixas@ci.uc.pt (J.S. Seixas de Melo).

¹ University of Milano-Bicocca, Department of Earth and Environmental Sciences, Milan, Italy

other paint objects, not yet studied, cannot be fully excluded.

Beyond **Shk** application as dyeing material, the curative and beneficial properties of gromwell root's extracts have been exploited since time in Traditional Chinese Medicine thought they have been just recently characterized. Indeed, it has been demonstrated that **Shk** presents antioxidant, anticancer, antidiabetic, anti-inflammatory and antimicrobial activity [4,13]. Additional studies on **Shk** and related molecules, have been carried out by Raman and SERS techniques [7,14,15], while its photophysical characterization has been performed in solution through UV-Vis spectroscopic techniques [16]. Moreover, the sensitivity of extracts of *Lithospermum erythrorhizon* to gamma irradiation has been also investigated [17].

Due to the interest in pharmacological field, some studies examined the thermal and photochemical degradation of shikonin [17-20]. The formation of a photo-oxidative product ((-)-5,8-dihydroxy-2-(1-hydroxy-3-oxo-4-methyl-4-pentenyl)-1,4-naphthoquinone) after one month of sun light exposure, whose structure retains the main skeleton of 5,8-dihydroxy-1,4-naphthoquinone, has been identified according to NMR, IR and FTIR data [18]. The effect of solvent polarity, pH and ionic strength on the photochemical decomposition of **Shk** in solution was also reported [19], together with a study on the stability towards light and temperature on the extracted dye [20]. However, concerning the basic knowledge of the **Shk** photochemistry, all the published works used polychromatic irradiation thus providing exclusively qualitative and comparative considerations. To have a deeper comprehension of shikonin's light sensitivity and to provide a univocal and quantitative description of its photoreaction efficiency, the determination of its quantum yield, using monochromatic light and accurately evaluating the fraction of absorbed light, would have to be performed.

Furthermore, in the case of **Shk**, literature lacks data on absorption and emission spectral information regarding changes induced by irradiation. On the other hand, it has been widely demonstrated that a noninvasive identification of natural dyes on artworks through UV-Vis spectroscopic techniques requires a deep knowledge of their spectral behavior in different media and under various environmental conditions [21,22]. Since exposure to light is one of the major causes of degradation of these colored substances in polychromatic works of art, it is essential to know how their spectral features evolve following irradiation. To fill this gap, in this paper a detailed study on the photophysical and photochemical behavior of **Shk** in solution and solid-state through UV-Vis absorption and fluorescence spectroscopy together with a quantitative determination of photoreaction quantum yield, is presented for the first time. To investigate the role of the different molecular moieties of **Shk** on the spectral changes induced by irradiation, three differently substituted naphthoquinones have also been investigated. The spectral characterization, both in absorption and emission, has been first carried out in solution and then to dye powder to monitor the eventual effect of aggregation on spectral behavior. Finally, paint mockups have been studied to evaluate potential modifications due to interactions of the dye with a micro-environment like what could be found in artwork. Moreover, the changes induced in the spectral properties of the dye by both poly- and monochromatic light have been investigated first in solution, the simplest environment in which peculiar and quantitative parameters can be obtained, and then in paint mockups where the information previously obtained in solution are extremely useful in evaluating similar and/or different properties related to the environment in which the dye is embedded. The photoproducts formed during irradiation experiments, most of them never detected, have been identified through high-performance liquid chromatography coupled with high resolution mass spectrometry (HPLC-HRMS).

2. Experimental section

2.1. Materials

Shikonin (**Shk**) and 5-hydroxy-1,4-naphthoquinone (**5HNQ**), were purchased from Sigma-Aldrich, whereas 5,8-dihydroxy-1,4-naphthoquinone (**DHNQ**) was from TCI and acetylshikonin (**AcShk**) from BOC Sciences. Barium sulfate with a purity of 99.998 % was obtained from Aldrich. Gum Arabic was obtained from Windsor & Newton and used dissolved in water to prepare the binder. All the materials were used without any further purification.

For the mock-up extraction for chromatographic analyses, ethylenediaminetetraacetic acid disodium salt (EDTA, Fluka, USA) and dimethylformamide (DMF; 99.8 % purity, J.T. Baker, USA) were used while PTFE syringe filters (4 mm thickness and 0.45 μm pore diameter, Agilent) were employed to filter the extract prior to chromatographic injection. The eluents for HPLC-ESI-Q-ToF were water and acetonitrile both LC-MS grade (Sigma Aldrich, USA) and added with 0.1 % v/v formic acid (FA; J.T. Baker, USA).

2.2. Solution samples preparation

A non-polar solvent, cyclohexane (Cx), and a polar protic solvent, ethanol (EtOH), were chosen and both solvents were spectroscopic grade. To detect photochemical changes induced by light exposure, solutions with absorbance values of ca. 1 were prepared. Prior to data acquisition, all samples were stirred to obtain a complete solubilization of the dye.

2.3. Solid samples preparation

The powder and paint mock-ups were both considered as solid samples. Powder samples were prepared by mixing the naphthoquinone dye with barium sulphate, with a BaSO₄:naphthoquinone (Ba:NQ) ratio of 96:4 w/w. Barium sulfate, having a negligible absorption in the UV-Vis spectral range, was chosen as a white non-luminescent medium to dilute the color of naphthoquinone powders to avoid saturation threshold in reflectance spectra and strong self-absorption in fluorescence profiles of NQs [23,24]. The paint layers were prepared by adding Arabic gum in a ratio of 85:15 (w/w) to the previously prepared powder mixture (Ba:NQ), and then a thin layer was cast on a polycarbonate plastic support.

2.4. Equipment

2.4.1. Absorption measurements

UV-Vis absorption spectra were recorded on a UV/Vis/NIR spectrophotometer (V-570 JASCO, Tokyo, Japan) equipped with Spectra Manager V-500 software. The spectra were acquired in the 200 – 800 nm range, with a 2 nm slit width; for the solution experiments, a 1 cm optical path length cuvette was used.

2.4.2. Fluorescence measurements

Fluorescence spectra were recorded using a Fluoromax⁺ spectrofluorometer (Horiba Scientific) using FluorEssence V3.9 software. The sample holder was adjusted according to the sample type, whether liquid or solid (powder and paint layer). All spectra were corrected for the instrumental response and acquired with a 3 and 10 nm spectral resolution for liquid and solid samples respectively. For the acquisition of emission spectra in solid state samples, different longwave pass filters were placed in front of the emission monochromator to avoid the entrance of reflected excitation light in it.

2.4.3. Reflectance measurements (portable equipment)

Reflectance measurements were performed using a portable spectrophotometer assembled as a prototype from separate Avantes

(Apeldoorn, The Netherlands) components already described in a previous paper [25] and equipped with a bifurcated quartz fiber optic system. The reflected light was collected at 21° respect to the surface, using a 0/0 geometry, thus avoiding most of the specular reflected light. A 99 % Spectralon® diffuse reflectance standard (Labsphere, North Sutton, USA) was used for calibration. The instrument provides an 8 nm spectral resolution whereas the fiber optic probe allows a surface area of about 2 mm² to be analyzed.

2.4.4. Light irradiance measurements

For all the poly- and mono-chromatic irradiation experiments performed an irradiance calibrated AvaSpec-2048-2 spectrometer (Avantes, NL) provided with a 200 μm diameter optical fiber (FC-UVIR200-2 ME, Avantes) and an 8 mm active area cosine corrector (CC-UV-VIS/NIR, Avantes) was employed. The spectrometer operates in the 200–1100 nm range (300 lines per mm grating) and is equipped with an AvaBench-75 optical bench, a 25 μm slit which produced 1.2 nm FWHM spectral resolution and a 2048-pixel CCD detector.

2.4.5. Irradiation procedure

This procedure is divided in three steps. First, the samples were irradiated with a xenon lamp filtered by a water and glass filter (the former cuts most of the infrared radiation thus preventing sample heating, the latter cuts off the UV-B light fraction) with a total irradiation time of approximately fourteen hours (14 h) producing a total irradiance exposure of 5.5×10^3 [Watt/cm²]. Air equilibrated solutions were irradiated in a capped cuvette (1 cm optical path length) without stirring. The changes induced in the absorption and emission properties were monitored in the same irradiated cuvette at each time interval by homogenizing solution before any spectral acquisition. This procedure was applied to all the compounds, in both cyclohexane and ethanol. For degraded samples, also a monochromatic irradiation experiment was performed to obtain a photo-degradation quantum yield (ϕ_R). This second irradiation experiment was performed using ultra-compact diode laser sources (Toptica Photonics AG, DE), providing different irradiation wavelengths, i.e. 375, 448, and 532 nm. All the samples were irradiated in both solvents for approximately sixteen hours (16 h) with a total irradiance exposure of 60 [Watt/cm²] for 375 nm, 1.2×10^3 [Watt/cm²] for 448 nm and 2.9×10^3 [Watt/cm²] for 532 nm. For the monochromatic irradiation experiments, the irradiated cuvette area was 0.28 cm², while for polychromatic experiments 0.38 cm². Third, an irradiation experiment was performed on the surface of the painting layer. The samples were placed in the same set-up used for polychromatic irradiation of solutions according to the first step and were irradiated for approximately eleven hours (11 h) with a total irradiance exposure of 4.3×10^3 [Watt/cm²].

2.4.6. Determination of photodegradation quantum yield

To be correctly quantified according to a reaction yield, a photoreaction must be studied in its initial phase when its degree of progress is limited and accessory secondary processes can be excluded.

Schematizing the process under study as a generic photoreaction:



where **A** is the reactant subjected to irradiation, and **B** is the photoproduct, the photoreaction quantum yield can be obtained by Eq. (1):

$$\phi_R = \frac{\text{number of B molecules formed}}{\text{number of photons absorbed by A}} \quad (1)$$

The first needed parameter, namely the number of photons absorbed by **A** during the irradiation time, is obtained by Eq. (2):

$$\text{Number of photons absorbed by A} = TNF \times F_{\text{isos nm}} \quad (2)$$

where TNF is the total number of photons per second that arrive to the

solution and F_{nm} is the fraction of light absorbed by **A**. The total number of photons can be obtained from the radiometric measurements, providing the number of photons per second, and the selected irradiation time, Δt , according to Eq. (3):

$$(TNF) = \frac{\text{n of photons}}{\text{sec}} \times \Delta t_{\text{sec}}^{\text{irradiation}} \quad (3)$$

The light fraction absorbed, F_{nm} , by **A** during the selected irradiation time, Δt , is obtained by the Eq. (4):

$$F_{\text{isos nm}} = (1 - 10^{-\overline{Abs}_{\text{isos nm}}}) \quad (4)$$

where \overline{Abs}^A is the average absorption of the reagent **A** at the irradiation wavelength. In the first step of the reaction, the decrease in concentration of the disappearing reactant **A** can be reasonably considered linear. Since the irradiation wavelength has been selected at the isobestic point (where both the reactant **A** and the photoproduct **B** have the same molar extinction coefficient), to have a constant total absorbance during the irradiation time, the $\overline{Abs}_{\text{isos}}^A$ can be obtained by the Eq. (5):

$$\overline{Abs}_{\text{isos}}^A = \frac{Abs_{\text{isos}}^{A,t=0} + Abs_{\text{isos}}^{A,t=i}}{2} \quad (5)$$

where $Abs_{\text{isos}}^{A,t=0}$ is the absorbance, at $t = 0$, of **A** at isobestic and, $Abs_{\text{isos}}^{A,t=i}$ is the absorbance, at $t = i$, of **A** at isobestic. Considering that one mole of **B** is formed for each mole of **A** reacted, $C_{\text{formed}}^B = C_{\text{reacted}}^A$, so the absorbance of **A** at the isobestic point at $t = i$ is obtained by Eq. (6):

$$Abs_{\text{isos}}^{A,t=i} = Abs_{\text{isos}}^{A,t=0} - Abs_{\text{isos}}^{B,t=i} = Abs_{\text{isos}}^{A,t=0} - (C_{t=i}^B \times \epsilon_{\text{isos}}) \quad (6)$$

Considering that in the spectral evolution we have the part at higher wavelength where only **A** absorbs, $C_{t=i}^B$ can be obtained in terms of decreasing in absorbance value of **A** after an irradiation time $t = i$ at the wavelength where only **A** absorbs (ΔAbs_{nm}^A) divided by the molar extinction coefficient of **A** at the same wavelength (ϵ_{nm}^A) according to the Eq. (7):

$$C_{t=i}^B = \frac{\Delta Abs_{nm}^A}{\epsilon_{nm}^A} \quad (7)$$

considering that, all the values of molar extinction coefficients of the reagent **A** are known values simply obtained from a quantitative absorption spectrum of **A** in the desired solvent.

The last experimental parameters needed for the quantum yield determination, namely the number of **B** molecules formed, is obtained by the Eq. (8):

$$\text{Number of B molecules formed} = C_{t=i}^B \times V_L^{\text{irradiated}} \times N \quad (8)$$

where $C_{t=i}^B$ is the concentration of **B** formed at $t = i$, $V_L^{\text{irradiated}}$ is the solution's irradiated volume in liters and, N is Avogadro's number.

2.4.7. High performance liquid chromatography coupled with high resolution mass spectrometry (HPLC-ESI-Q-ToF)

An HPLC 1200 Infinity coupled to a Jet Stream ESI-Q-ToF 6530 Infinity detector, and equipped with an Agilent Infinity autosampler (Agilent Technologies, Palo Alto, CA, USA) was used. MassHunter® Workstation Software (B.04.00) was used to carry out instrument control, data acquisition and analysis. The mass spectrometer operated in ESI negative ionization mode and the working conditions were: drying gas N₂ (purity >98 %) temperature 350 °C and 10 L/min flow; nebulizer gas pressure 35 psi; capillary voltage 4.5 KV; sheath gas temperature 375 °C and 11 L/min flow; fragmentor voltage 175 V; nozzle voltage 1000 V; skimmer voltage 1000 V; octapole RF voltage 750 V. High resolution MS and MS/MS spectra were acquired in negative mode in the range 100 – 1700 m/z at 1.04 spectra/sec scan rate (CID voltage 30 V, collision gas N₂, purity 99.999 %). The FWHM (Full Width Half Maximum) of

quadrupole mass bandpass used during MS/MS precursor isolation was 4 *m/z*. Auto-calibration was performed daily using Agilent tuning mix HP0321 (Agilent Technologies) prepared in acetonitrile.

The chromatographic separation was performed on an analytical reversed-phase column Poroshell 120 EC—C18 (3.0 × 75 mm, particle size 2.7 μm,) with a pre-column Zorbax (4.6 × 12.5 mm, particle size 5 μm) both Agilent Technologies (Palo Alto, CA, USA). The eluents were A: formic acid (FA 0.1 % v/v) in water and B: formic acid (FA 0.1 % v/v) in acetonitrile. The flow rate was 0.4 mL/min. The program was as follow: 15 % B for 2.6 min, then to 50 % B in 13.0 min, to 70 % B in 5.2 min, to 100 % B in 0.5 min and then hold for 6.7 min; re-equilibration took 11 min. During the separation the column was thermostated at 30 °C. The injection volume was 5 μL.

The ethanol extracts were filtered with PTFE syringe filters (0.45 μm) and then injected in the chromatographic systems without any dilution.

3. Results and discussion

The spectral characteristics (absorption and emission maxima together with Stokes shifts values) of the studied naphthoquinone molecules before irradiation, are listed in Table 1; data in cyclohexane can be found in ref [16]. The reported results and the relative **Shk** spectra displayed in Fig. 1 (in ethanol) and Fig S11 (in cyclohexane) show that the absorption and emission features and the Stokes shift do not change significantly in relation to solvent, within the spectral resolution.

The photodegradation study of shikonin (**Shk**) and of model hydroxynaphthoquinone dyes, 5-hydroxynaphthoquinone (**5HNQ**), 5,8-dihydroxy-1,4-naphthoquinone (**DHNQ**), and acetylshikonin (**AcShk**) (Scheme 1) was performed. The molecules were irradiated with xenon polychromatic source (with spectral distribution close to the solar spectrum, see Section 2.4.5) in organic solvents, cyclohexane (Cx) and ethanol (EtOH). To estimate the photo-degradation reaction quantum yield (ϕ_R), monochromatic irradiation experiments were also performed at 375 nm, 448 nm, and 532 nm in the two organic solvents. These specific wavelengths correspond to the isosbestic points observed in the absorption spectral evolutions obtained under polychromatic irradiation; they have been chosen because the total absorbed light does not change during the selected irradiation time. Furthermore, in the first step of the reaction the light is absorbed only by the starting naphthoquinone molecule. Finally, the solid-state characterization of the powder and a polychromatic irradiation experiment of paint mock-ups were undertaken.

The reaction kinetics was monitored by acquiring the UV–Vis absorption / reflectance and fluorescence emission spectra of both solution and paint layers. The resulting photoproducts detected in **Shk** solutions and in painting layer extracts were further characterized by HPLC–ESI–Q–ToF.

3.1. Photochemical behavior of Shikonin and naphthoquinones parent compounds in solution

The spectral evolution of **Shk** in EtOH under 14 h of polychromatic light exposure (inset a) compared with those under dark conditions (inset c) are reported in Fig. 1. The absorption band of **Shk** in the range 450 – 600 nm decreases as the irradiation proceeds (orange arrow in

Table 1

Absorption ($\lambda_{Abs, max}$) and fluorescence emission ($\lambda_{Em, max}$) wavelength maxima (nm) and Stokes shift (Δ_{SS} , cm^{-1}) of 5HNQ, DHNQ, Shk and AcShk, in ethanol.

Compound/solvent	EtOH		
	$\lambda_{Abs, max}$	$\lambda_{Em, max}$	Δ_{SS}
5HNQ	424	613	7272
DHNQ	519	618	3087
Shk	516	618	3199
AcShk	519	622	3191

Fig. 1a) while a broad absorption feature at 330 – 450 nm increases (a gray arrow in Fig. 1a). Three isosbestic points at 221 nm, 285 nm and 442 nm are maintained over the first 8 h of irradiation indicating the formation of a single photoproduct. In the subsequent hours of light exposure, the isosbestic points are not preserved suggesting the formation of other different photoproducts.

As far as the fluorescence behavior is concerned, by exciting at $\lambda_{exc} = 400$ nm and 516 nm, a progressive intensity reduction of the long wavelength emission band (orange arrow in Fig. 1b) – due to the reducing absorption of the chromophore – and a concomitant increase of the short wavelength emission band (gray arrow in Fig. 1b) – likely ascribable to the formation of photo-product(s) – resulting from light exposure, are observed. A similar behavior is also noticed in Cx, for **Shk**, Fig. S11. On the contrary, in the dark, no relevant changes in the absorption spectra are detected (Fig. 1c), whereas small modifications in the fluorescence profiles are experienced (Fig. 1d), negligible with respect to the high variations observed under light exposure. This difference should be attributed to the increased sensitivity of spectrofluorimetry compared to spectrophotometry.

A plot of the variation of **Shk** absorbance and fluorescence emission intensity as a function of irradiation time at different wavelengths is shown in Fig. 2. The same experiment but performed under dark conditions (acting as a control), shows that the absorption and fluorescence emission values remain constant over time, regardless of the solvent used. On the other hand, upon light exposure, the maximum absorbance and emission values of the chromophore decrease while those of the possible photoproduct(s) increase. In particular, the absorbance of **Shk**, after ca. 5 h irradiation halves regardless of the solvent (see Fig. 2a for Cx at ■522 nm, and Fig. 2b for EtOH at ■517 nm).

Quite similar spectral changes were observed when **5HNQ** and **AcShk** solutions were exposed to polychromatic light irradiation in both EtOH and Cx (see Figures S12 to S15) whereas no significant changes were detected for **DHNQ** (Figs. S16 and S17). Peculiar is the behaviour of **5HNQ** in EtOH (Fig. S12), where the absorption and emission features of the chromophore almost disappear after 12 h of irradiation, indicating a lower stability of this molecule to polychromatic light. In Cx (Fig. S13), in contrast to EtOH (Fig. S12), the intensity of emission spectra increase, especially as regards the band at lower emission wavelength (with maxima at ~ 460 nm). This does not happen for **Shk** (Fig. 1 for EtOH and Fig. S11 for Cx) and for **AcShk**, where in EtOH (Fig. S14) and in Cx (Fig. S15) there is a similar behaviour with irradiation, i.e. an increase of the lowest emission band with irradiation. These data seem to indicate that **5HNQ** has a different behaviour, especially in EtOH, compared to the other hydroxynaphthoquinone derivatives studied.

The so far obtained results leads to assume that the studied molecules follow an equivalent photochemical pathway except for **DHNQ** that shows higher stability to light irradiation. This stability is due to the six membered ring, involving the hydroxy and carbonyl group in close proximity, which facilitate a very fast Excited State Intramolecular Proton Transfer (ESIPT) reaction. This is common to other hydroxy-carbonyl systems such as 3-hydroxyflavone derivatives [26–28]; yet, it does not necessarily involves a six membered ring, but a close proximity between OH (or NH) and C = O groups [22,29]. This ESIPT, which also acts as a very effective radiationless deactivation channel, although present in all compounds, appears to be more effective in **5HNQ** than in **Shk**, **AcShk**, as reflected by the lower fluorescence quantum yield of **5HNQ** and the high internal conversion quantum yield of the diacetylated compound (99 %) [16].

To obtain the photo-degradation quantum yield (ϕ_R), solutions of the studied compounds were exposed to monochromatic irradiation with wavelengths corresponding to the isosbestic points observed in the absorption profiles attained under polychromatic irradiation (375 nm only for **5HNQ**, 448 nm and 532 nm). The calculated values (Table 2) are quite low (in the range 10^{-4} – 10^{-5}) for all the studied naphthoquinone derivatives indicating low efficiency of the primary photochemical event. The values for **DHNQ** were not determined since the absorbance

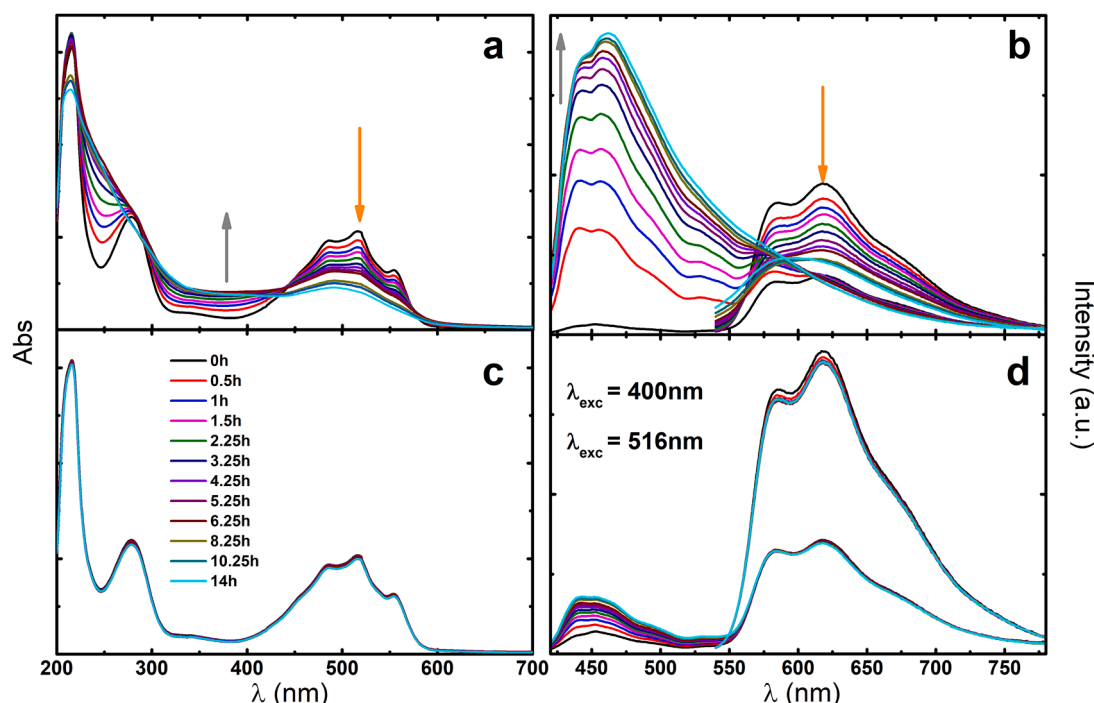
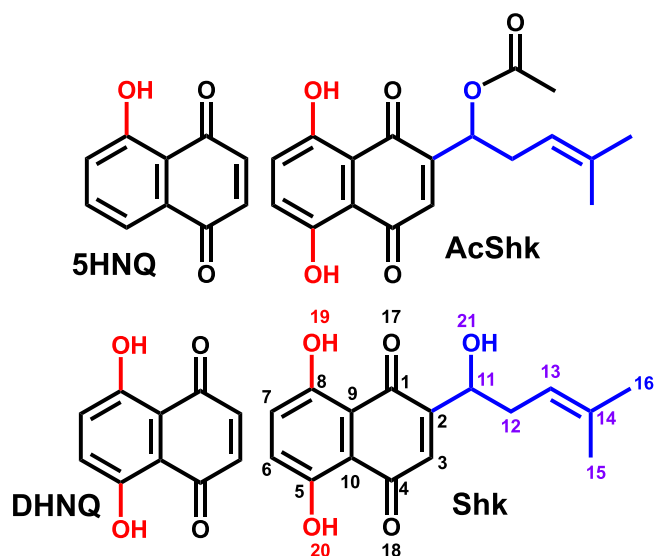


Fig. 1. Left-hand column, absorption (a, c) spectra and right-hand column, fluorescence emission (b, d) spectra acquired for **Shk** in ethanol at different time intervals, and with excitation wavelength (λ_{exc}) of 400 and 516 nm. The spectra c and d were obtained under dark conditions while the spectra a and b, under polychromatic irradiation.



Scheme 1. Chemical structures and acronyms of shikonin (**Shk**), 5-hydroxy-naphthoquinone (**5HNQ**), 5,8-dihydroxy-1,4-naphthoquinone (**DHNQ**), and acetylshikonin (**AcShk**). For **Shk** numbering of the carbon atoms is showed.

variations induced by polychromatic light were negligible with respect to those of other compounds: the molecule can be considered stable. In all conditions (different solvents and excitation wavelengths) **Shk** displays the lowest ϕ_R values (in all cases 10^{-5}), whereas **5HNQ** has photoreaction quantum yields one order of magnitude higher than the parent molecules (Table 2).

For comparison, a photochemical study performed on indigotin in the presence of oxygen, reported ϕ_R values of about 10^{-4} [30]. In general, the spectral trend in absorption and emission observed during the experiments in monochromatic light is the same as that detected by irradiating with polychromatic light, but the changes observed are much

more contained due to the lower intensity of incident (and consequently of absorbed) light. As an example, spectral changes induced by monochromatic irradiation of **Shk** in EtOH are reported in Fig. S18.

3.2. Photochemical behavior of Shikonin and naphthoquinones parent compounds in the solid state

To investigate if changes in micro-environment can play a role in determining the photophysical and photochemical behavior of the studied naphthoquinones (NQ), polychromatic experiments were also performed on powders and paint mockups. **Shk**, **5HNQ**, **DHNQ** and **AcShk** were first mixed with barium sulfate to “dilute” /attenuate the color intensity. This is needed to avoid the signal reaching a saturation level when reflectance spectra are collected and to minimize self-absorption contribution in fluorescence signals [23,24]. Arabic gum was chosen as a binder for the preparation of paint layers due to its low, or even negligible, absorption and emission contribution in the spectral range explored during irradiation experiments. Furthermore, unlike other binders, it neither undergoes polymerization or cross-linking nor interacts significantly with the dye, thus minimizing any binder interference on the degradation study of the dye.

Finally, considering the above-mentioned hypothesis of **Shk** as pigment, the painting on paper is the most common technique in which organic natural dyes have been applied without being precipitated or mixed with additives, and in which natural gums have been commonly used as binders. Fig. 3 shows the absorption (k/s values) and fluorescence spectra of the studied compounds in $\text{BaSO}_4\text{:NQ}$ blends and in $\text{BaSO}_4\text{:NQ:gum}$ Arabic pictorial layers before light irradiation. No significant differences have been observed for the two studied systems except for a slight bathochromic shift in absorption profiles of **5HNQ** and **DHNQ** mockups with respect to the corresponding powder blends. Moreover, although the spectra are characterized by broader and less structured shapes than those observed for the same dyes in solution, the positions of the absorption and emission maxima neither change significantly nor new bands are observed. This indicates that the photophysical behavior of the studied dyes in the solid state and in pictorial

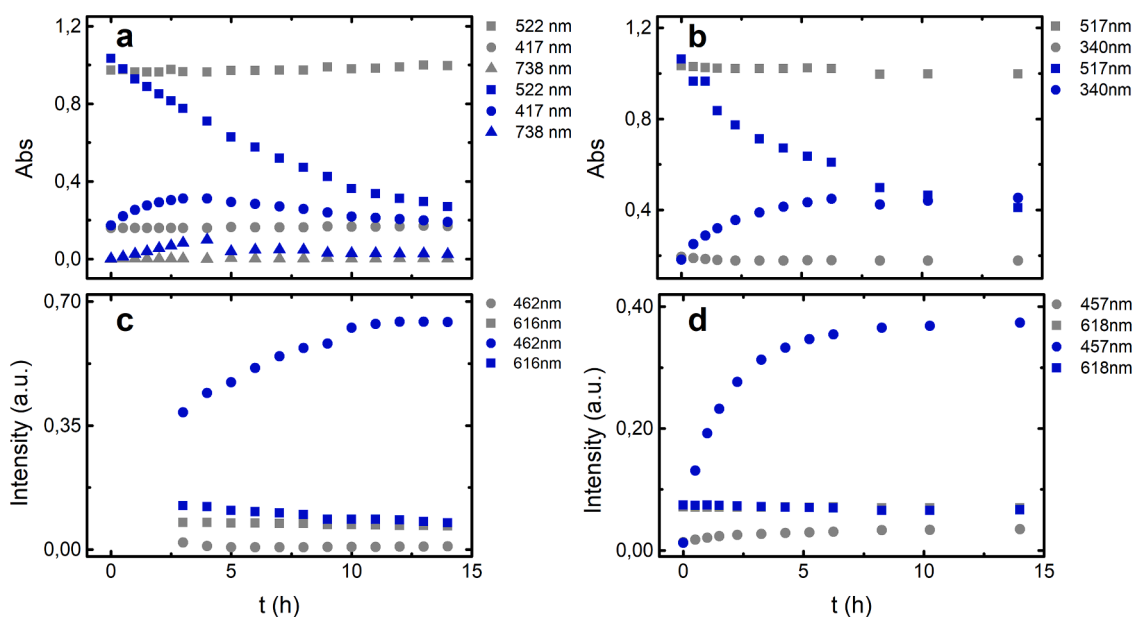


Fig. 2. Variation of the absorbance (a, b) and fluorescence emission intensity (c, d) at different wavelengths versus irradiation time for **Shk** in cyclohexane (a, c) and ethanol (b, d), obtained under dark conditions (gray dots and squares) and irradiation (blue dots, squares, and triangles) conditions.

Table 2

Photodegradation quantum yield (ϕ_R) values obtained for **5HNQ**, **Shk** and **AcShk** in **Cx** and **EtOH**, at different light exposure wavelengths (λ_{irr}): 375, 448 and 532 nm.

Solvent	λ_{irr}	5HNQ	Shk	AcShk
Cx	375	7.49×10^{-4}	–	–
	448	1.03×10^{-4}	1.57×10^{-5}	1.60×10^{-4}
	532	–	1.92×10^{-5}	6.37×10^{-5}
EtOH	375	3.63×10^{-4}	–	–
	448	3.84×10^{-4}	7.03×10^{-5}	6.58×10^{-5}
	532	–	2.59×10^{-5}	2.94×10^{-5}

layer closely resemble that observed in solution. This experimental evidence suggests that the chemical interaction of each studied dye with itself and with the binder is very poor.

Photo-aging of the pictorial mockups was carried out under polychromatic light irradiation over approximately 12 h. The Kubelka-Munk and the fluorescence emission spectra at different irradiation times (shown in Fig. 4 for **Shk**) do not show a regular trend as was instead observed in solution (Figs 1 and 2).

This behavior, very common in the solid state, is generally ascribed to a superficial inhomogeneity of the sample and difficulty in recording spectra exactly on the same spot at each irradiation time interval. However, similarly to what was found in solution, the polychromatic irradiation of paint mock-ups globally leads to an increase of absorption in the blue wavelength range (Fig. 4a) and, at the same time, to the appearance of a new emission band at shorter wavelengths (Fig. 4b). In fact, the fluorescence emission spectra, acquired with $\lambda_{exc} = 470$ nm (Fig. 4), shows a decrease of the chromophore fluorescence band centered at ca. 650 nm (orange arrow Fig. 4b) with a concurrent increase (marked with the gray arrow, centered at ca. 550 nm) of a fluorescence emission ascribable to the formed photoproduct(s). Thus, when exposed to light, **Shk** presents a similar behavior regardless of the chemical environment. Light irradiation induces the degradation of **Shk** and the formation of photoproduct(s) characterized by specific absorption and fluorescence emission bands always detected at lower wavelength values compared to those of the starting dye. This agrees with mass spectrometric data that allowed the identification of the same photoproducts both in solution and in solid state (see Section 3.3).

3.3. Characterization by HPLC-ESI-Q-ToF of the photoproducts of **Shk** formed in solution and in the paint layers

To perform the characterization of the photoproduct(s) by HPLC-ESI-Q-ToF, four solutions of **Shk** in EtOH, non-irradiated (and stored in the dark) and irradiated with polychromatic light for different time intervals (1 h, 3 h and 5 h) in which the isobestic points are maintained, were analyzed. Despite the presence of the isobestic point in the spectral evolution, the following described results highlight the presence of several products, suggesting a more complex reaction pathways for **Shk** compared to what already described in the literature.

In Fig. 5, the HPLC-ESI-Q-ToF Extract Ion Chromatograms (EICs) of the molecular ions of **Shk** and the four identified photoproduct(s) from the extracts of non-irradiated and 5 h – irradiated samples, are displayed.

Table 3 summarizes all compounds detected in the different extracts. This includes **Shk** [15,31] and photoproduct(s) mass data and different tentative formula for the same molecular ion. Some of the hypothesized products (**p1** – **p4**) retain the same naphthoquinone core of **Shk** and they just differ for modifications relative to the linear chain bound to C2 (double bonds and oxygen atoms), however open structures implying the breakdown of the naphthoquinone backbone cannot be excluded.

Keeping in mind that the naphthoquinone core is responsible for the color of **Shk** [16], and that spectral data collected for **Shk** solutions discussed in the previous sections suggest the formation of a photoproduct(s) absorbing at lower wavelength, further analyses based on preparative chromatography and NMR techniques would be necessary to unequivocally assign the chemical structures of the detected products. Nevertheless, because the only verified data present in literature concerning the photoreactivity of **Shk** has demonstrated the presence of the product labeled as **p1** (Table 3), namely the 5,8-dihydroxy-2-(1-hydroxy-3-oxo-4-methyl-4-pentenyl)-1,4-naphthoquinone [18], we can suggest a similar structure also for all the other products.

Fig. 6, presents the integrated areas in the Extract Ion Chromatograms (EIC) for **p1-p4** and **Shk** compounds in the extracts of the standard Shikonin solution stored in the dark and aged for 1 h, 3 h and 5 h. To visualize a tentative kinetic trend of the evolution of the degradation products, areas relative to **Shk** and **p1** – **p4** were integrated in the Extract Ion Chromatograms (EIC) of the four extracts (Fig. 5), and the obtained values plotted against the irradiation time in the graph

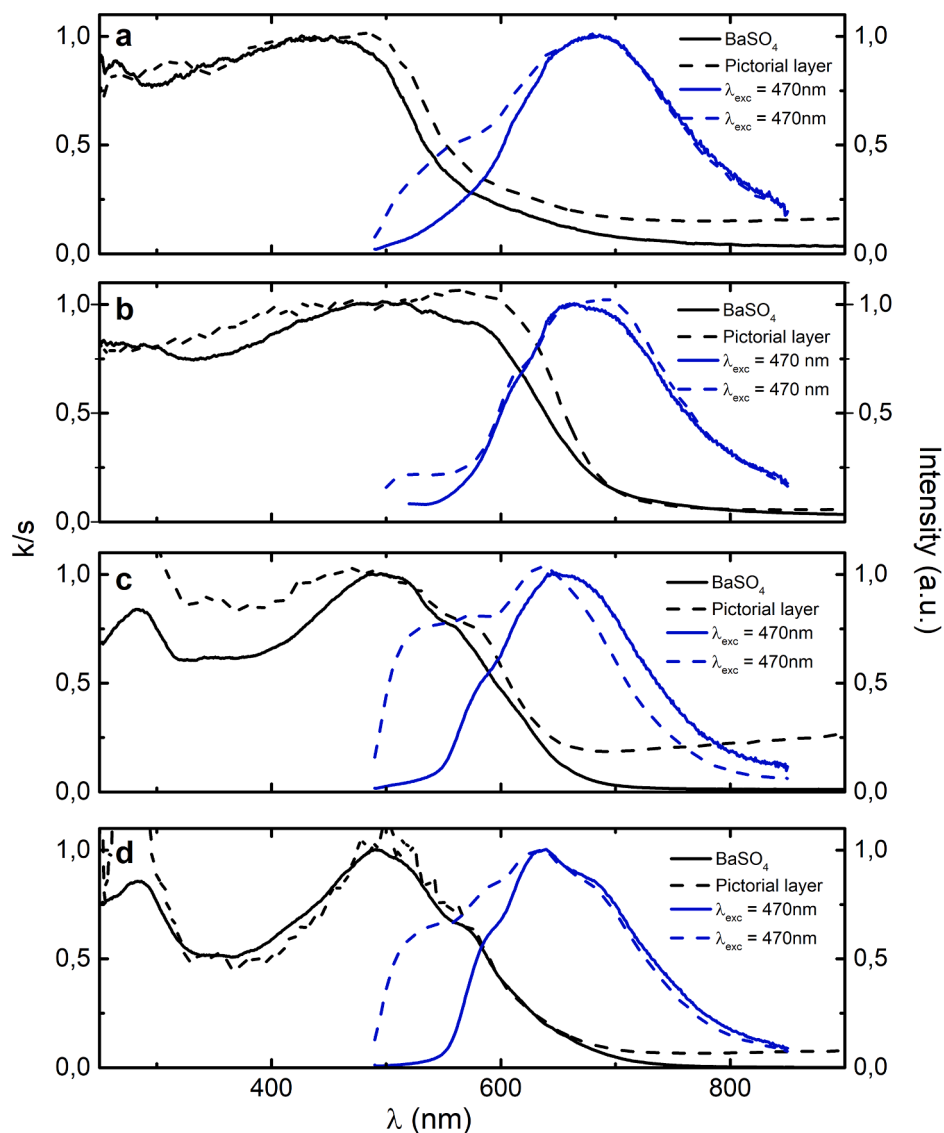


Fig. 3. Normalized Kubelka-Munk and fluorescence emission spectra relative to (a) 5HNQ, (b) DHNQ, (c) Shk and (d) AcShk, in BaSO₄ (solid line,—) and to paint mock-up (dashed line, - - -), acquired at $\lambda_{exc} = 470$ nm. The shoulder at about 510 nm observed on emission spectra of paint mockups is a spectral distortion due to the use of a long-pass wavelength filter placed in front of the emission monochromator.

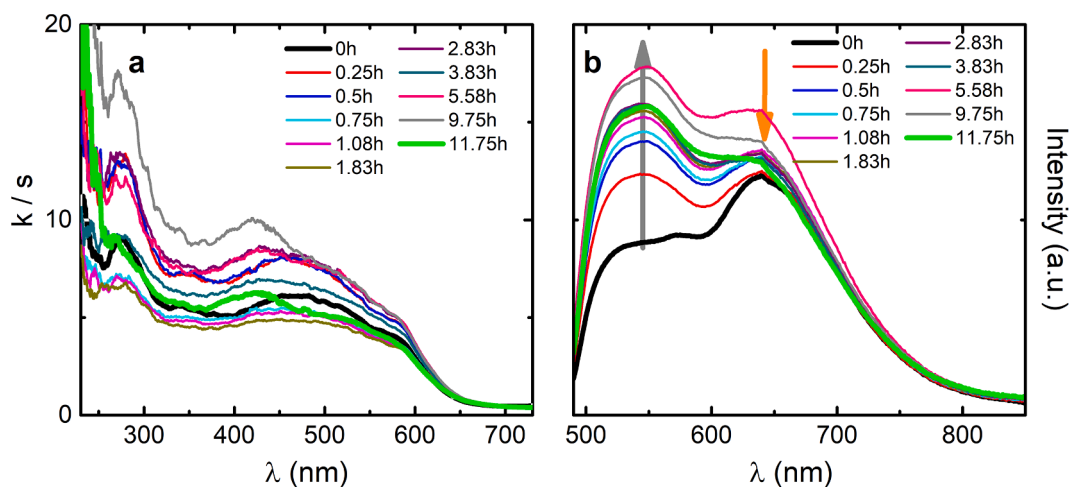


Fig. 4. Kubelka-Munk (a) and fluorescence emission spectra (b) acquired at $\lambda_{exc} = 470$ nm, obtained for Shk pictorial layer during the irradiation procedure.

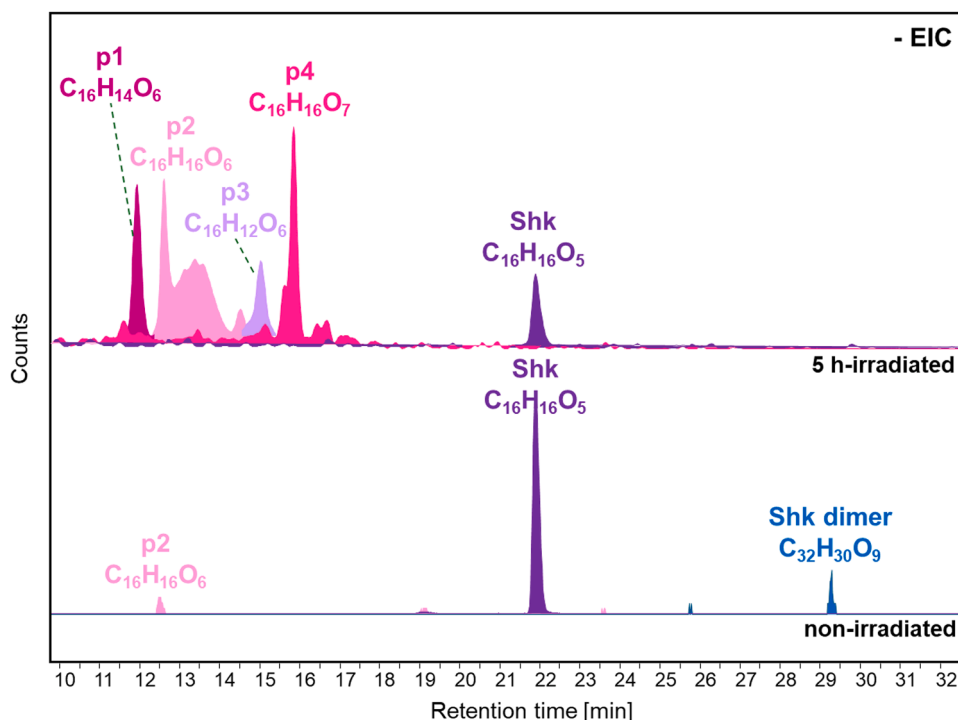


Fig. 5. HPLC-ESI-Q-ToF Extract Ion Chromatogram (EIC) of **p1** ($C_{16}H_{14}O_6$), **p2** ($C_{16}H_{16}O_6$), **p3** ($C_{16}H_{12}O_6$), **p4** ($C_{16}H_{16}O_7$), **Shk** ($C_{16}H_{16}O_5$) and **Shk dimer** ($C_{32}H_{30}O_9$) from the extracts of non-irradiated and 5 h - irradiated sample. Negative acquisition mode.

reported in Fig. 6. The graph shows as the EIC area of **Shk** decreases with time, in accordance with what observed on artificially aged silk dyed with *Lithospermum erythrorhizon* [3]. Other products (**p2**, **p3** and **p4**) are formed within the first hour of irradiation and then tend to decrease: this is the typical behavior of intermediate products. Conversely, **p1** tends to increase up to a plateau.

The analysis of the non-irradiated paint mock-up extract presents only one of the photoproducts identified in solution (**p2**), while for those irradiated for 3 h and 5 h, a broad peak ascribable to a dehydrogenated form of **Shk** dimer (**DHShk** dimer, $C_{32}H_{28}O_9$) is clearly evident in the chromatogram, along with **p1**, **p2** and **p3** (Fig.SI11). Moreover, **Shk** dimer ($C_{32}H_{30}O_9$), already described in the literature as a component of *Lithospermum erythrorhizon* raw material [32], was detected in traces in the extract of the non-irradiated solution. Possible oxidation reactions occurring in solution during the irradiation experiment may be responsible for the cleavage of **Shk** dimeric form explaining its absence in the irradiated extracts chromatograms. On the contrary, in the solid state it is plausible suggesting oxygen diffusion occurs slowly with respect to solution. Radical cross-coupling might be the responsible for the formation of dimeric forms such as **DHShk** dimer, detected in the 16h - irradiated mockup.

Summarizing at this stage: exposure of **Shk** solutions to polychromatic light leads in few hours to a remarkable reduction of the main absorption band of the chromophore with a concomitant increase of an absorption at shorter wavelengths. These changes, in line with fading phenomena in other solvents under similar irradiation conditions reported in the literature [17-20,33,34], earned **Shk** the reputation of unstable or labile molecule. A similar behavior has been observed on paint mockups in agreement with browning reported on textiles dyed with gromwell [33]. In apparent contrast, the here obtained photo-degradation quantum yields (ϕ_R) in solution showed very low values, further suggesting that **Shk** should be a very stable molecule, regardless the solvent and the irradiation wavelengths. The value retrieved for this molecule is even lower than that reported for indigotin that is considered one of the most stable compounds amongst natural dyes [29,35]. A tentative reasonable explanation for this apparent

contrast could be found in the complex evolution of the photo-degradation pathway which this natural dye undergoes. Indeed, from HPLC-ESI-Q-ToF, the identification of 6 products (**p1-p4**, **Shk-dimer** and **DH-Shk-dimer**) in solution was obtained, with 5,8-dihydroxy-2-(1-hydroxy-3-oxo-4-methyl-4-pentenyl)-1,4-naphthoquinone (**p1**) showing a kinetic trend of a final product. Indeed, analysis of the overall data, reveals that the first part of the Shikonin photoreaction leads to, apparently, formation of a single photoproduct, in agreement with the presence of some isosbestic points in the spectral evolution. The low measured quantum yield value refers to this part of the reaction. As the reaction proceeds, the isosbestic points are lost and the HPLC-MS measurements highlight the formation of several different reaction products, some of them showing intermediate behaviors. During the irradiation, the amount of those photoproducts, after an initial rise, decreases forming other chemical compounds. This is evident when polychromatic light is used, possibly due to efficient absorption of light by the photoproducts which, in turn, can further react leading to the formation of new species. This evolution subtracts several products to the whole reaction inducing an increase of the **Shk** disappearance efficiency. For these reasons, the starting photochemical event, first consequence of the light absorbed by **Shk**, has a low efficiency in agreement with the low quantum yield determined, while the presence of several photoproducts, which actively participate to the whole reaction pathway and disappearing during the irradiation time, induce an efficient fading of the starting Shikonin dye.

4. Conclusion

By using absorption and emission spectroscopies, and liquid chromatography coupled with mass spectrometry the photodegradation behavior of **Shk** was investigated both in solution and in the solid state, including powder and paint mock-ups providing a wide overview on spectral changes induced by irradiation. The structure of several photoproducts was herein proposed. The non-invasive diagnostic for organic dyes in cultural heritage objects is often based on their absorption and emission spectral features. In this work, we showed that the loss of

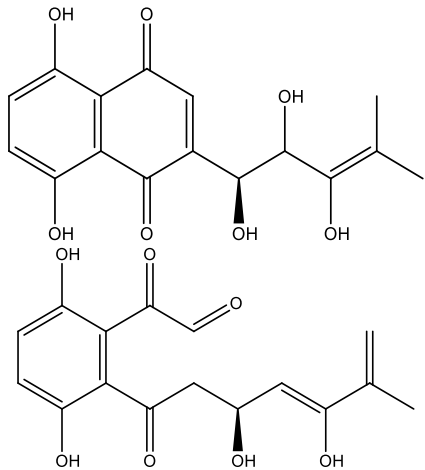
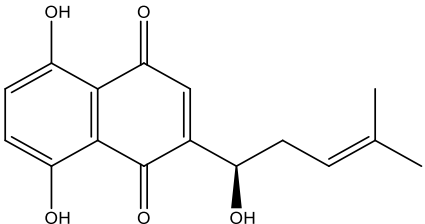
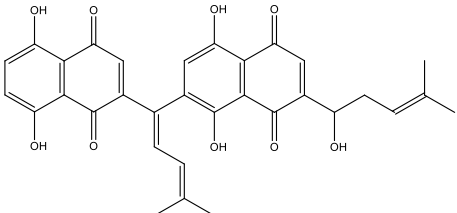
Table 3

List of the compounds detected in the extracts together with the relative tentative structures, retention time, molecular formula, precursor ion and product ion. Product ions highlighted in bold represent the more intense signals in the tandem mass spectrum.

Compound	Tentative structure	Retention time (min)	Molecular formula	Precursor ion	Product ions
p1		11.8	C ₁₆ H ₁₄ O ₆	301.07	130.965 146.959 176.011 189.017 204.004 217.048 233.009 241.050 255.054 273.076 286.047
p2		12.6	C ₁₆ H ₁₆ O ₆	303.087	130.965 205.016 233.008
p3		15.2	C ₁₆ H ₁₂ O ₆	299.056	108.022 118.375 136.524 157.027 176.011 196.898 213.023 225.054 238.057 254.053
p4		15.7	C ₁₆ H ₁₆ O ₇	319.082	130.965 161.024 173.021 189.019 203.032 215.034 227.035 243.031 269.042 287.056 302.082

(continued on next page)

Table 3 (continued)

Compound	Tentative structure	Retention time (min)	Molecular formula	Precursor ion	Product ions
Shk		21.9	C ₁₆ H ₁₆ O ₅	287.092	173.018 190.020 218.014 [1]
Shikon dimer-H ₂ (DHShk)		27.1	C ₃₂ H ₂₈ O ₉	555.168	402.038 443.042 486.096
Shk dimer		29.3	C ₃₂ H ₃₀ O ₉	557.182	470.100 419.043 298.087

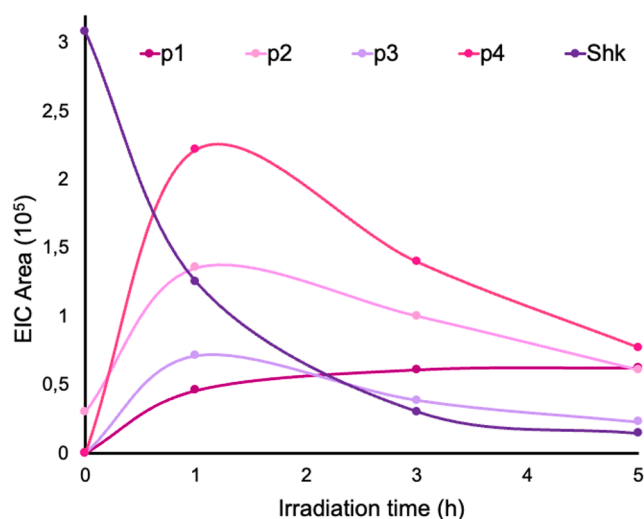


Fig. 6. Integrated areas in the Extract Ion Chromatograms (EIC) for **p1**, **p2**, **p3**, **p4** and **Shk** compounds in the extracts of the standard **Shk** solution in EtOH stored in the dark, aged for 1 h, 3 h and 5 h. The area for **Shk** was divided by 10 to enhance clarity, and the points were interpolated (no mathematical fitting was performed) for easier visualization of the trends in all the compounds. Since analytical standards of **p1-p4** are not available, only semi-quantitative analyses can be carried out.

the spectral structure and the overall band broadening makes the identification of **Shk** through its characteristic absorption features very difficult through UV-Vis absorption/reflectance spectroscopy. Thus, the absorption and emission properties of the photoproducts generated by the irradiation of **Shk** characterized for the first time in this study, could be potentially very useful for indirect evidence of **Shk** in degraded art objects. Furthermore, the obtained basic knowledge of the dye's behavior is fundamental for ongoing studies concerning other classic historical uses of natural dyes, such as the production of lake pigment and textile dyeing.

Supporting Information

Supplementary Figures S11 to S111 are provided as a Source Data File.

CRediT authorship contribution statement

C.M. Pinto: Writing – original draft, Visualization, Investigation, Formal analysis. **C. Clementi:** Writing – review & editing, Writing – original draft, Validation, Investigation, Formal analysis, Conceptualization. **F. Sabatini:** Writing – review & editing, Investigation, Formal analysis. **I. Degano:** Writing – review & editing, Methodology, Formal analysis. **A. Romani:** Writing – review & editing, Methodology, Conceptualization. **J.S. Seixas de Melo:** Writing – review & editing, Writing – original draft, Supervision, Investigation, Funding acquisition, Conceptualization.

Declaration of competing interest

The authors declare that they have no known competing financial interests or personal relationships that could have appeared to influence the work reported in this paper.

Data availability

Data will be made available on request.

Acknowledgment

We acknowledge financial support from CQC-IMS which is supported by the Portuguese Agency for Scientific Research, “Fundação para a Ciência e Tecnologia” (FCT) through the projects UIDB/00313/2020 (<https://doi.org/10.54499/UIDB/00313/2020>) and UIDP/00313/2020 (<https://doi.org/10.54499/UIDP/00313/2020>) and the Institute of Molecular Sciences (IMS) through special complementary funds provided by FCT. CMP also acknowledges FCT for a PhD grant (SFRH/BD/140883/2018 and COVID/BD/153285/2023).

Supplementary materials

Supplementary material associated with this article can be found, in the online version, at [doi:10.1016/j.molstruc.2024.138898](https://doi.org/10.1016/j.molstruc.2024.138898).

References

- X. Chen, L. Yang, N. Zhang, J.A. Turpin, R.W. Buckheit, C. Osterling, J. J. Oppenheim, O.M. Howard, Shikonin, a component of chinese herbal medicine, inhibits chemokine receptor function and suppresses human immunodeficiency virus type 1, *Antimicrob. Agents Chemother* 47 (9) (2003) 2810–2816.
- C.K.K. Choo, K.S. Lau, Y.E. Lee, Analysis of dyeings produced by traditional Korean methods using colorants from plant extracts, *Colorat. Techn.* 118 (1) (2002) 35–45.
- D. Tamburini, Investigating Asian colourants in Chinese textiles from Dunhuang (7th–10th century AD) by high performance liquid chromatography tandem mass spectrometry – Towards the creation of a mass spectra database, *Dyes. Pigm.* 163 (2019) 454–474.
- S. Yadav, A. Sharma, G.A. Nayik, R. Cooper, G. Bhardwaj, H.S. Sohal, V. Mutreja, R. Kaur, F.O. Areche, M. AlOudat, A.M. Shaikh, B. Kovács, A.E. Mohamed Ahmed, Review of shikonin and derivatives: isolation, chemistry, biosynthesis, pharmacology and toxicology, *Front. Pharmacol* 13 (2022).
- J.H.H. de Graaff, W.G.T. Roelofs, M.R. van Bommel, The colourful past: origins, chemistry and identification of natural dyestuffs, *Abegg-Stiftung*, 2004.
- D. Cardon, Natural dyes: sources, tradition, technology and science, *Archetype*, 2007.
- M.V. Cañameres, M.G. Mieites-Alonso, M. Leona, Raman, SERS and DFT analysis of the natural red dyes of Japanese origin alkanin and shikonin, *Mole. Biomole. Spectrosc.* 265 (2022) 120382.
- R. Laursen, Yellow and red dyes in ancient asian textiles, in: E.b.M.M.D.a.M. Bethé (Ed.), *Color in ancient and medieval East Asia*, Spencer Museum of Art, the University of Kansas, Lawrence, 2015, pp. 81–92.
- W. Cheng, History of textile technology of ancient China, Science Press, New York, 1992. Science Press Rego Park, NY, [Beijing], Rego Park, NY, [Beijing].
- M.M. Dusenbury, Color at the Japanese court in the asuka and nara periods, in: E.b. M.M.D.a.M. Bethé (Ed.), *Color in ancient and medieval East Asia*, Spencer Museum of Art, the University of Kansas, Lawrence, 2015, pp. 123–134.
- I. Degano, L. Triolo, S. Conti, Beyond the eye-sight: the puzzle of a Japanese Manchira, *e-Preservat. Sci.* 10 (2013) 19–26.
- D. Tamburini, C.R. Cartwright, M. Pullan, H. Vickers, An investigation of the dye palette in chinese silk embroidery from dunhuang (Tang dynasty), *Archaeol. Anthropol. Sci.* 11 (4) (2019) 1221–1239.
- C. Guo, J. He, X. Song, L. Tan, M. Wang, P. Jiang, Y. Li, Z. Cao, C. Peng, Pharmacological properties and derivatives of shikonin—A review in recent years, *Pharmacol. Res.* 149 (2019) 104463.
- E. De Luca, M. Redaelli, C. Zaffino, S. Bruni, A SERS and HPLC study of traditional dyes from native Chinese plants, *Vib Spectrosc* 95 (2018) 62–67.
- K. Kato, B. Doherty, I. Degano, F. Sabatini, C. Miliani, A. Romani, K. Ito, B. G. Brunetti, An SERS analytical protocol for characterizing native Japanese plant extracts, *J. Raman Spectrosc.* 51 (6) (2020) 892–902.
- C.M. Pinto, J. Pina, E. Delgado-Pinar, J.S. Seixas de Melo, Excited state deactivation mechanisms in Shikonin rationalized from its naphthoquinone parent structures, *Phys. Chem. Chem. Phys.* 24 (34) (2022) 20348–20356.
- M.H. Lee, Y.R. Moon, J.-H. Kim, I.-C. Lee, K.-S. Lee, B.Y. Chung, J.-Y. Cho, Differential radiation sensitivity of shikonin derivatives from Lithospermum erythrorhizon S, *J. Korean Soc. Appl. Biol. Chem.* 53 (6) (2010) 724–728.
- H.-W. Cheng, F.-A. Chen, H.-C. Hsu, C.-Y. Chen, Photochemical decomposition of alkanin/shikonin enantiomers, *Int. J. Pharm.* 120 (2) (1995) 137–144.
- F.-A. Chen, H.-W. Cheng, A.-B. Wu, H.-C. Hsu, C.-Y. Chen, Kinetic studies of the photochemical decomposition of alkanin/shikonin enantiomers, *Chem. Pharm. Bull.* 44 (1) (1996) 249–251.
- M.-H. Cho, Y.-S. Paik, T.-R. Hahn, Physical stability of shikonin derivatives from the roots of lithospermum erythrorhizon cultivated in Korea, *J. Agric. Food Chem.* 47 (10) (1999) 4117–4120.
- A. Romani, C. Zuccaccia, C. Clementi, An NMR and UV–visible spectroscopic study of the principal colored component of Stil de grain lake, *Dyes Pigments* 71 (3) (2006) 218–223.
- R. Rondão, J.S. Seixas de Melo, J. Pina, M.J. Melo, T. Vitorino, A.J. Parola, Brazilwood Reds: the (Photo)chemistry of Brazilin and Brazilin, *J. Phys. Chem. A* 117 (41) (2013) 10650–10660.
- C. Clementi, C. Miliani, G. Verri, S. Sotiropoulou, A. Romani, B.G. Brunetti, A. Sgamellotti, Application of the Kubelka–Munk correction for self-absorption of fluorescence emission in carmine lake paint layers, *Appl. Spectrosc.* 63 (12) (2009) 1323–1330.
- P.L. Gentili, C. Clementi, A. Romani, Ultraviolet–visible absorption and luminescence properties of Quinacridone–barium sulfate solid mixtures, *Appl. Spectrosc.* 64 (8) (2010) 923–929.
- C. Clementi, B. Doherty, P.L. Gentili, C. Miliani, A. Romani, B.G. Brunetti, A. Sgamellotti, Vibrational and electronic properties of painting lakes, *Appl. Phys. A* 92 (1) (2008) 25–33.
- S. Ameer-Beg, S.M. Ormson, R.G. Brown, P. Matousek, M. Towrie, E.T.J. Nibbering, P. Fogg, F.V.R. Neuwahl, Ultrafast measurements of excited state intramolecular proton transfer (ESIPT) in room temperature solutions of 3-hydroxyflavone and derivatives, *J. Phys. Chem. A* 105 (15) (2001) 3709–3718.
- M. Itoh, K. Tokumura, Y. Tanimoto, Y. Okada, H. Takeuchi, K. Obi, I. Tanaka, Time-resolved and steady-state fluorescence studies of the excited-state proton-transfer in 3-hydroxyflavone and 3-hydroxychromone, *J. Am. Chem. Soc.* 104 (15) (1982) 4146–4150.
- G.J. Woolfe, P.J. Thistlethwaite, Direct observation of excited-state intramolecular proton-transfer kinetics in 3-hydroxyflavone, *J. Am. Chem. Soc.* 103 (23) (1981) 6916–6923.
- J.S. Seixas de Melo, The molecules of colour. The real blue indigo: photostability mechanisms, new functional derivatives, and hybrids, in: S. Crespi, S. Protti (Eds.), *Photochemistry: Volume 49*, The Royal society of chemistry, 2022, pp. 31–52.
- M.M. Sousa, C. Miguel, I. Rodrigues, A.J. Parola, F. Pina, J.S. Seixas de Melo, M. J. Melo, A photochemical study on the blue dye indigo: from solution to ancient Andean textiles, *Photochem. Photobiol. Sci.* 7 (11) (2008) 1353–1359.
- M. Liao, A. Li, C. Chen, H. Ouyang, Y. Zhang, Y. Xu, Y. Feng, H. Jiang, Systematic identification of shikonins and shikonofurans in medicinal Zicao species using ultra-high performance liquid chromatography quadrupole time of flight tandem mass spectrometry combined with a data mining strategy, *J. Chromatogr. A* 1425 (2015) 158–172.
- A.N. Assimpoulou, M. Ganzera, H. Stuppner, V.P. Papageorgiou, Simultaneous determination of monomeric and oligomeric alkanin and shikonins by high-performance liquid chromatography-diode array detection-mass spectrometry, *Biomed. Chromatogr.* 22 (2) (2008) 173–190.
- D. Tamburini, J. Dyer, T. Heady, A. Derham, M. Kim-Marandet, M. Pullan, Y.-P. Luk, I. Ramos, Bordering on Asian paintings: dye analysis of textile borders and mount elements to complement research on asian pictorial art, *Heritage* 4 (4) (2021) 4344–4365.
- V.P. Papageorgiou, A.N. Assimpoulou, E.A. Couladouros, D. Hepworth, K. C. Nicolaou, The chemistry and biology of alkanin, shikonin, and related naphthazarin natural products, *Angewandte Chemie Internat. Edit.* 38 (3) (1999) 270–301.
- J.S. Seixas de Melo, The Molecules of Colour, in: A. Albini, E. Fasani, S. Protti (Eds.), *Photochemistry*, The royal society of chemistry, London, 2018, pp. 68–100.